Domanda estratta n. 3

Domande riguardanti l'argomento specifico

1. whole-exome sequencing: utilizzo in oncologia, pipelines/tools principali, files di output

2. RNA-seq: utilizzo in oncologia, pipelines/tools principali, files di output

3. Deconvoluzione immunitaria da bulk RNA-seq: a cosa serve e quali sono i principali tools

Domanda estratta n. 3

DOMANDE INFORMATICA

1. Descrivere i principali programmi del pacchetto Office

2. Cos'è un database?

3. Che cos'è il backup?

Domanda estratta n. 3

ESMO GOOD SCIENCE BETTER MEDICINE BEST PRACTICE

ANNALS OF ONCOLOGY driving innovation in oncology

ORIGINAL ARTICLE

Clonal *KEAP1* mutations with loss of heterozygosity share reduced immunotherapy efficacy and low immune cell infiltration in lung adenocarcinoma

S. Scalera[1†], B. Ricciuti[2†], M. Mazzotta[3†], N. Calonaci[4], J. V. Alessi[2], L. Cipriani[1], G. Bon[5], B. Messina[6], G. Lamberti[2], A. Di Federico[2], F. Pecci[2], S. Milite[4], E. Krasniqi[7], M. Barba[7], P. Vici[8], A. Vecchione[9], F. De Nicola[1], L. Ciuffreda[1], F. Goeman[1], M. Fanciulli[1], S. Buglioni[10], E. Pescarmona[10], B. Sharma[11], K. D. Felt[11], J. Lindsay[12], S. J. Rodig[11,13], R. De Maria[14,15], G. Caravagna[4], F. Cappuzzo[7], G. Ciliberto[16], M. M. Awad[2‡] & M. Maugeri-Saccà[6,7*‡]

[1]SAFU Laboratory, Department of Research, Advanced Diagnostic, and Technological Innovation, IRCCS Regina Elena National Cancer Institute, Rome, Italy; [2]Lowe Center for Thoracic Oncology, Dana-Farber Cancer Institute, Harvard Medical School, Boston, USA; [3]Medical Oncology Unit, Sandro Pertini Hospital, Rome; [4]Department of Mathematics and Geosciences, University of Trieste, Trieste; [5]Cellular Network and Molecular Therapeutic Target Unit, IRCCS Regina Elena National Cancer Institute, Rome; [6]Clinical Trial Center, Biostatistics and Bioinformatics Division, IRCCS Regina Elena National Cancer Institute, Roma; [7]Division of Medical Oncology 2, IRCCS Regina Elena National Cancer Institute, Rome; [8]UOSD Phase IV Studies, IRCCS Regina Elena National Cancer Institute, Rome; [9]Department of Clinical and Molecular Medicine, Pathology Unit, Sant'Andrea Hospital, Sapienza University, Rome; [10]Department of Pathology, IRCCS Regina Elena National Cancer Institute, Rome, Italy; [11]ImmunoProfile, Brigham & Women's Hospital and Dana-Farber Cancer Institute, Boston; [12]Knowledge Systems Group, Dana-Farber Cancer Institute, Boston; [13]Department of Pathology, Brigham and Women's Hospital, Boston, USA; [14]Dipartimento di Medicina e Chirurgia Traslazionale, Università Cattolica del Sacro Cuore, Rome; [15]Fondazione Policlinico Universitario A. Gemelli IRCCS, Rome; [16]Scientific Direction, IRCCS Regina Elena National Cancer Institute, Rome, Italy

Available online 13 December 2022

Background: *KEAP1* mutations have been associated with reduced survival in lung adenocarcinoma (LUAD) patients treated with immune checkpoint inhibitors (ICIs), particularly in the presence of *STK11/KRAS* alterations. We hypothesized that, beyond co-occurring genomic events, clonality prediction may help identify deleterious *KEAP1* mutations and their counterparts with retained sensitivity to ICIs.

Patients and methods: Beta-binomial modelling of sequencing read counts was used to infer *KEAP1* clonal inactivation by combined somatic mutation and loss of heterozygosity (*KEAP1* C-LOH) versus partial inactivation [*KEAP1* clonal diploid-subclonal (*KEAP1* CD-SC)] in the Memorial Sloan Kettering Cancer Center (MSK) MetTropism cohort ($N = 2550$). Clonality/LOH prediction was compared to a streamlined clinical classifier that relies on variant allele frequencies (VAFs) and tumor purity (TP) (VAF/TP ratio). The impact of this classification on survival outcomes was tested in two independent cohorts of LUAD patients treated with immunotherapy (MSK/Rome $N = 237$; DFCI $N = 461$). Immune-related features were studied by exploiting RNA-sequencing data (TCGA) and multiplexed immunofluorescence (DFCI mIF cohort).

Results: Clonality/LOH inference in the MSK MetTropism cohort overlapped with a clinical classification model defined by the VAF/TP ratio. In the ICI-treated MSK/Rome discovery cohort, predicted *KEAP1* C-LOH mutations were associated with shorter progression-free survival (PFS) and overall survival (OS) compared to *KEAP1* wild-type cases (PFS log-rank $P = 0.001$; OS log-rank $P < 0.001$). Similar results were obtained in the DFCI validation cohort (PFS log-rank $P = 0.006$; OS log-rank $P = 0.014$). In both cohorts, we did not observe any significant difference in survival outcomes when comparing *KEAP1* CD-SC and wild-type tumors. Immune deconvolution and multiplexed immunofluorescence revealed that *KEAP1* C-LOH and *KEAP1* CD-SC differed for immune-related features.

Conclusions: *KEAP1* C-LOH mutations are associated with an immune-excluded phenotype and worse clinical outcomes among advanced LUAD patients treated with ICIs. By contrast, survival outcomes of patients whose tumors harbored *KEAP1* CD-SC mutations were similar to those with *KEAP1* wild-type LUADs.

Key words: lung cancer, immunotherapy, *KEAP1*, clonal mutations, loss of heterozygosity

INTRODUCTION

The Kelch-like ECH-associated protein 1- nuclear factor erythroid 2 -related factor 2 (KEAP1-NRF2) pathway maintains cellular redox homeostasis and protects cells from xenobiotics.[1-3] Under basal conditions, KEAP1 mediates the proteasomal degradation of NRF2 via the Cullin 3 - RING-box protein 1 ubiquitin ligase complex. Redox, metabolic, or xenobiotic

*Correspondence to: Dr Marcello Maugeri-Saccà, Clinical Trial Center, Biostatistics and Bioinformatics Division, IRCCS Regina Elena National Cancer Institute, Via Elio Chianesi 53, 00144, Roma, Italy. Tel: +39-0652662724; Fax: +39-0652665523

E-mail: marcello.maugerisacca@ifo.it (M. Maugeri-Saccà).

†These authors contributed equally to this work.

‡These authors share senior authorship.

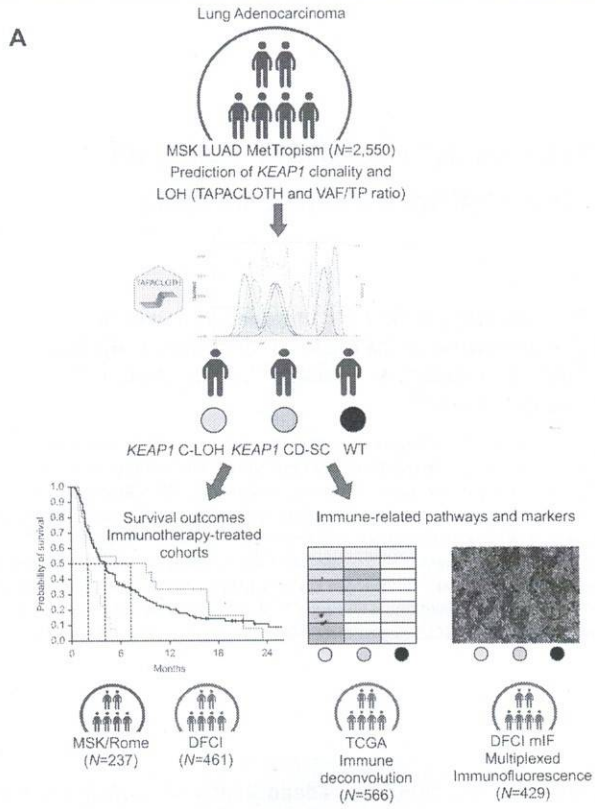

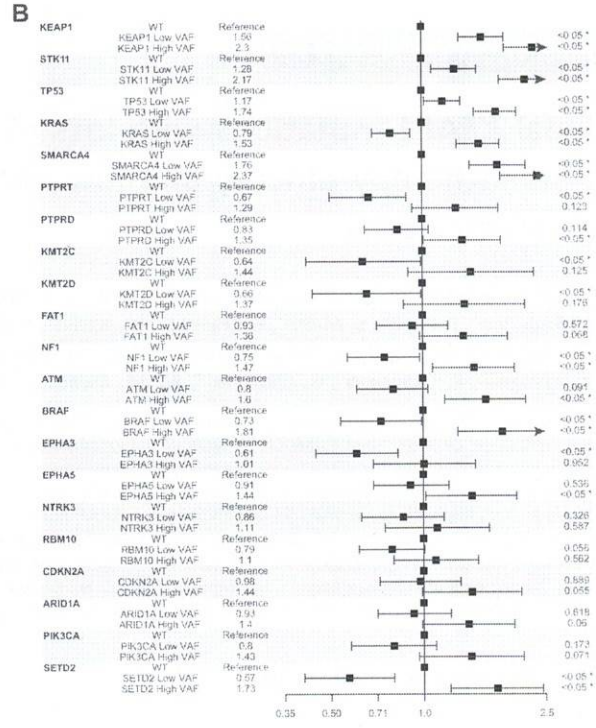

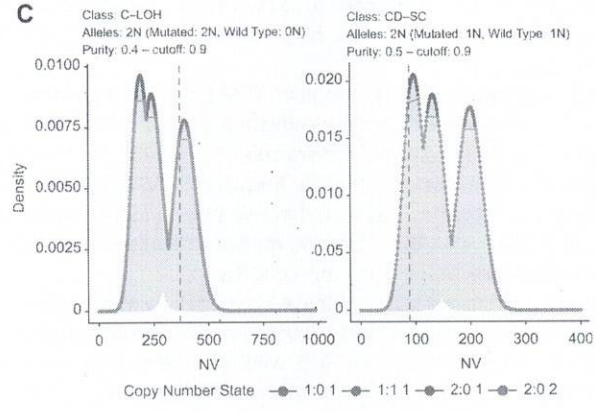

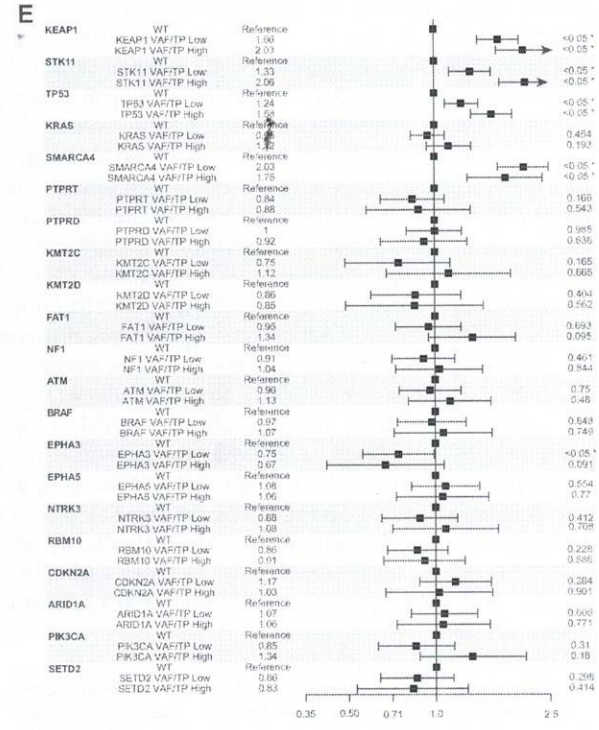

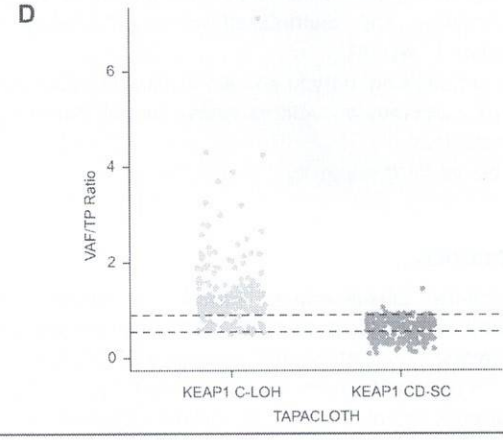

stressors produce modifications in KEAP1 sensor cysteines, hindering its capability to target NRF2 for degradation. When NRF2 is released from the inhibitory effects of KEAP1, it dimerizes with small musculoaponeurotic fibrosarcoma proteins and triggers the expression of target genes. The transcriptional output of NRF2 activation aims at re-establishing the redox homeostasis, extruding chemicals, and preventing ferroptosis.[1-3] Functional experiments and computational studies have also revealed that the KEAP1-NRF2 axis is connected to the antitumor immune response.[4-9]

KEAP1-NFE2L2 (the gene encoding for NRF2) mutations occur in 20%-25% of lung adenocarcinoma (LUAD).[10-12] Moreover, *KEAP1* loss of heterozygosity (LOH) was described in LUAD, indicating that a certain fraction of tumors is characterized by complete abrogation of protein function.[13] *KEAP1* mutations have been associated with chemoresistance and radioresistance,[14,15] as well as reduced sensitivity to epidermal growth factor receptor (EGFR)-targeted inhibitors and compounds targeting the RTK-RAS-MAPK pathway.[16,17] Likewise, *KEAP1* is investigated in the domain of LUAD immunotherapy, relying on mutational co-occurring models denoting functional gene interactions. The most noteworthy examples refer to the co-existence of *KEAP1* and *KRAS/STK11/SMARCA4* alterations,[8,18] the neutral relationship between *KEAP1* and *TP53* mutations,[9] and the mutual exclusivity with *EGFR* mutations.[8]

A deeper understanding of the disease stemmed from whole-exome/genome sequencing studies (WES/WGS). Large-scale genome data allow to reconstruct the clonal composition of tumors and their evolutionary trajectories.[19-22] Mathematical modelling of these processes relies on a set of genomic features including tumor purity (TP, the percentage of neoplastic cells in a tumor sample), variant allele frequency (VAF, the number of variant reads divided by the number of total reads, reported as a percentage), allele-specific copy number alterations (CNAs: LOH and amplifications), and ploidy. Clinical targeted sequencing is usually considered suboptimal for this type of inference given the limited throughput. Nevertheless, TP and VAF, which are central in clonal deconvolution, are routinely assessed in clinical sequencing.

We hypothesized that the combined evaluation of these two parameters may predict *KEAP1* inactivation status, namely, clonal *KEAP1* mutations with LOH versus conditions of partially retained function (clonal diploid or subclonal mutations). To address this question, we conceived the following workflow: (i) The MSK MetTropism cohort was used to explore the relationship between VAF and TP. *KEAP1* clonality/LOH prediction was carried out leveraging a statistical framework generated for this study (TAPACLOTH), and its performances were compared with a clinically focused classifier that relies on VAF and TP (VAF/TP ratio); (ii) The impact of the different *KEAP1* mutations was tested in two cohorts of LUAD patients treated with immune checkpoint inhibitors (ICIs) (discovery cohort: MSK/Rome; validation cohort: DFCI); and (iii) Immunological correlates were investigated using whole-transcriptome sequencing (WTS, TCGA) and multiplexed immunofluorescence (DFCI mIF cohort).

PATIENTS AND METHODS

Cohorts and patients

Survival analyses were carried out in two independent cohorts of advanced LUAD patients who received programmed cell death (ligand) - 1 [PD-(L)1] inhibitors. The MSK/Rome discovery cohort included 237 advanced LUAD patients assessable for overall survival (OS) who received ICIs. An independent validation of the model was carried out in the DFCI cohort, consisting of 461 metastatic LUAD patients treated with immunotherapy. Overall, we identified 698 patients evaluable for OS who underwent tissue-based next-generation sequencing (tNGS), and 631 patients evaluable for progression-free survival (PFS). 1

The MSK/Rome discovery cohort was profiled with MSK-IMPACT341/410/468 panels[23,24] and the FoundationOne®CDx assay.[8] The DFCI validation cohort was profiled with the DFCI-Oncopanel-2/3.[18] TP was prevalently estimated by pathologists (MSK and DFCI cases, $N = 672$). Regarding samples profiled by the FoundationOne®CDx assay ($N = 26$), we exploited computational TP. In this case, computational TP and VAFs were requested to the manufacturer for the specific purposes of this study (https://info.foundationmedicine.com/hubfs/FMI%20Labels/FoundationOne_CDx_Label_Technical_Info.pdf). The cohorts considered for exploratory and computational analyses (MSK MetTropism, TCGA), inclusion/exclusion criteria, and IRB approval are provided as Supplementary Methods, available at https://doi.org/10.1016/j.annonc.2022.12.002.

Statistical and bioinformatic analyses

Survival curves were estimated with the Kaplan–Meier product-limit method and compared using the log-rank test. Multivariate Cox regression models were generated with variables potentially impacting survival outcomes (OS and PFS), taking into account their availability in the original 2

Figure 1. **Relationship between variant allele frequency and tumor purity in the MSK MetTropism study.** Graphical representation of the study workflow (A). Forest plot illustrating univariate Cox regression analyses for OS related to top-mutant genes classified according with VAFs (B). Asterisks indicate statistically significant differences. The highest tertile was used as the cut-off point (high versus low VAFs). TAPACLOTH-based prediction of clonality and loss of heterozygosity (C). Two representative *KEAP1*-mutant cases are illustrated: clonal with LOH (*KEAP1* C-LOH, left) and clonal diploid/subclonal (*KEAP1* CD-SC, right). Methodological details are provided in the 'Methods' section. Dot plot showing the overlap between clonality/LOH inference (TAPACLOTH) and the VAF/TP ratio (D). Dotted lines indicate VAF/TP tertiles. Forest plot illustrating univariate Cox regression analyses for OS comparing high versus low TP-adjusted VAFs (VAF/TP ratio of top-ranking mutant genes), defined on the basis of the highest tertile (E). Asterisks indicate statistically significant differences.
CD-SC, clonal diploid-subclonal; DFCI, Dana-Farber Cancer Institute; LOH, loss of heterozygosity; LUAD, lung adenocarcinoma; OS, overall survival; MSK, Memorial Sloan Kettering Cancer Center; NV, number or reads with variant; TP, tumor purity; VAF, variant allele frequency; WT, wild-type.

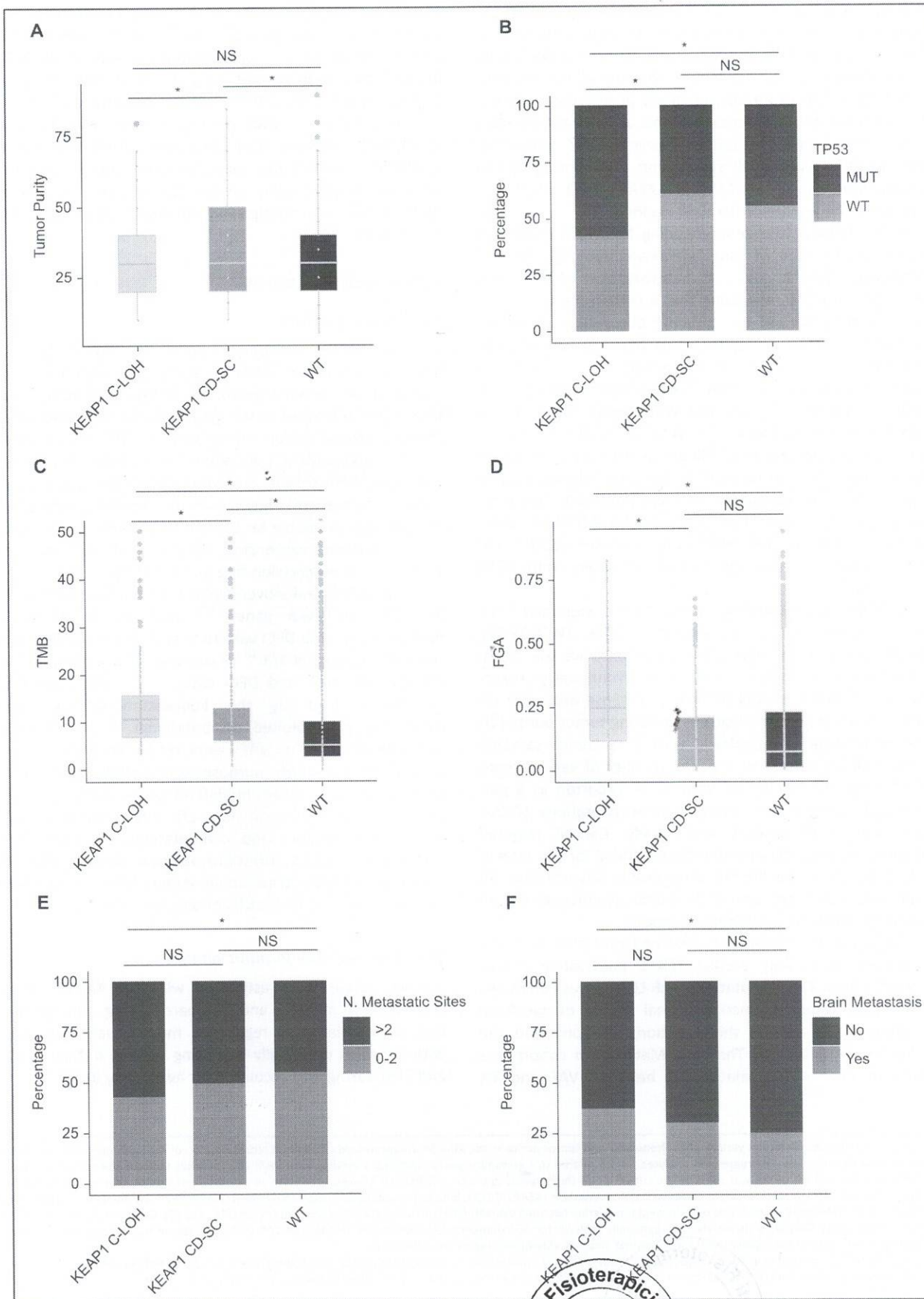

datasets. The related estimates were reported as hazard ratio and 95% confidence interval. Immunogenomic data (TCGA LUAD) were downloaded from open-source data portals (https://www.cri-iatlas.org/resources/; and http://science.bostongene.com/tumor-portrait).[25,26] Additional statistical and bioinformatic analyses are described in the Supplementary Methods, available at https://doi.org/10.1016/j.annonc.2022.12.002.

Classification of *KEAP1* mutations

The MSK MetTropism LUAD cohort was used to predict *KEAP1* clonality/LOH with TAPACLOTH, a model that we have developed to work with read count data of clinical targeted sequencing (R package: https://caravagnalab.github.io/TAPACLOTH/). TAPACLOTH uses a beta-binomial or binomial likelihood based on the number of observed reads with the variant allele, against the total number of reads. These two measurements determine the VAF adopted in the test of this study, and are combined in TAPACLOTH by considering TP (further details are provided as Supplementary Methods, available at https://doi.org/10.1016/j.annonc.2022.12.002).

In order to generate a simplified classifier for routine clinical use, we compared TAPACLOTH with a method based on VAFs and TP. We exploited the VAF/TP ratio, hypothesizing that *KEAP1* mutations with VAFs similar to the respective TP were those sharing clonality and LOH. Given that in the MSK MetTropism cohort TAPACLOTH and the VAF/TP ratio obtained comparable results, the VAF/TP method was applied to survival analyses to ensure feasibility in the clinical setting. The highest tertile of the VAF/TP ratio was used to classify *KEAP1* mutations as clonal with LOH (*KEAP1* C-LOH) or clonal diploid-subclonal (*KEAP1* CD-SC) across all the cohorts considered. This choice stemmed from the comparison of TAPACLOTH and the VAF/TP ratio in the MSK MetTropism cohort (see 'Results' section).

Multiplexed immunofluorescence (ImmunoProfile)

Multiplexed immunofluorescence (mIF) was carried out on DFCI samples by staining 5-micron formalin-fixed, paraffin-embedded whole tissue sections with standard, primary antibodies sequentially and paired with a unique fluorochrome followed by staining with nuclear counterstain/4′, 6-diamidino-2-phenylindole (DAPI).[27] Samples were stained for PD-L1 (clone E1L3N), programmed cell death protein 1 (PD-1) [clone EPR4877(2)], CD8 (clone 4B11), FOXP3 (clone D608R), cytokeratin (clone AE1/AE3), and DAPI. Further details are provided as Supplementary Methods, available at https://doi.org/10.1016/j.annonc.2022.12.002.

RESULTS

Clonality/LOH prediction in clinical targeted sequencing

The workflow of this study is illustrated in Figure 1A. In reasoning that VAFs may provide hints on the clonal status of a given mutation, we tested the association between VAFs and OS in advanced LUAD patients in the MSK MetTropism ($N = 2550$). For the majority of the genes tested (mutational frequency $\geq 5\%$), we noticed that mutations occurring at high VAFs (highest tertile) were associated with an increased risk of death (Figure 1B and Supplementary Table S1, available at https://doi.org/10.1016/j.annonc.2022.12.002), suggesting the existence of a confounding factor. In particular, we observed that elevated TP estimates were associated with inferior OS (Supplementary Figure S1A, available at https://doi.org/10.1016/j.annonc.2022.12.002). Since TP was positively correlated with VAFs (Supplementary Figures S1B and S2, available at https://doi.org/10.1016/j.annonc.2022.12.002), we concluded that the detrimental effect of raw VAFs on clinical outcomes is a function of the TP.

Thus, we explored alternative avenues to introduce the concept of clonality/LOH in clinical sequencing. By focusing on *KEAP1*, we conceived TAPACLOTH to classify mutations as *KEAP1* C-LOH, and *KEAP1* CD-SC (Figure 1C). When TAPACLOTH prediction was compared to a streamlined clinical classification model defined by the VAF/TP ratio, we observed that the VAF/TP ratio efficiently intercepted TAPACLOTH-predicted *KEAP1* clonality/LOH (Figure 1D). Indeed, the majority of putative *KEAP1* C-LOH mutations clustered within the highest tertile of the VAF/TP ratio (Figure 1D). Next, we applied the VAF/TP ratio to the same pool of genes previously tested on a VAF basis only. With this approach, the negative prognostic impact was exclusively retained by established tumor-suppressor genes (Figure 1E and Supplementary Table S2, available at https://doi.org/10.1016/j.annonc.2022.12.002), indicating that our method accurately discriminates between relevant genomic alterations and clinically neutral events.

We next sought to identify potential differences across *KEAP1* C-LOH, *KEAP1* CD-SC, and *KEAP1* wild-type cases. As expected, the VAF/TP method limited baseline imbalances in tumor cellularity (Figure 2A). Mutation enrichment analysis revealed that the *KEAP1* C-LOH group was enriched for *TP53* mutations (Figure 2B), while *STK11* and *KRAS* mutations were similarly distributed between the two *KEAP1*-mutant groups (Supplementary Figure S3, available at https://doi.org/10.1016/j.annonc.2022.12.002). In addition, both the tumour mutational burden (TMB) TMB and the fraction of genome altered (FGA) were significantly higher in *KEAP1* C-LOH tumors as compared to *KEAP1* CD-SC and wild-type LUADs (Figure 2C and D). From a clinical perspective, tumors with *KEAP1* C-LOH mutations were

Figure 2. **Genomic and clinical features associated with the different *KEAP1* mutations in the MSK MetTropism study.** Box plot for TP in the three subgroups of interest (*KEAP1* C-LOH, *KEAP1* CD-SC, and *KEAP1* wild-type) (A). Stacked bar chart showing the distribution of *TP53* mutations in *KEAP1* C-LOH, *KEAP1* CD-SC, and *KEAP1* wild-type tumors (B). Box plots for tumor mutational burden (C) and FGA (D). Stacked bar chart displaying the distribution of metastatic burden (number of metastatic sites) (E) and brain metastases (F) across the three subsets of interest. Asterisks indicate statistically significant differences. CD-SC, clonal diploid-subclonal; C-LOH, clonal with loss of heterozygosity; FGA, fraction of genome altered; MSK, Memorial Sloan Kettering Cancer Center; MUT, mutated; NS, not significant; TP, tumor purity; WT, wild-type.

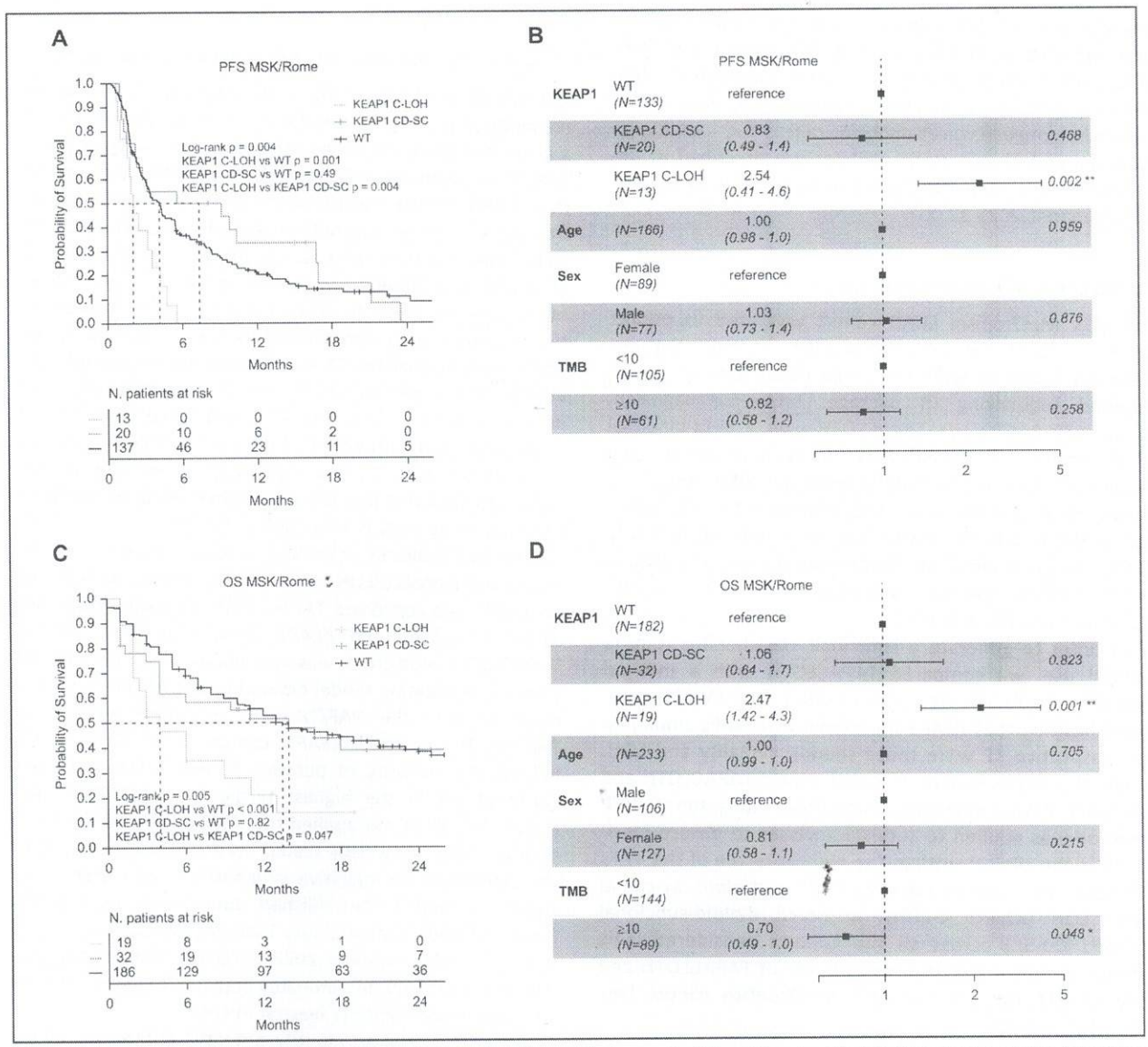

Figure 3. **Survival analyses in the MSK/Rome and DFCI cohorts.** Kaplan–Meier survival curves for PFS and OS, and multivariate Cox regression analyses, in the MSK/Rome cohort (A-D). Kaplan–Meier survival curves and multivariate Cox regression analyses (PFS and OS) in the DFCI validation cohort (E-H).
CD-SC, clonal diploid-subclonal; C-LOH, clonal with loss of heterozygosity; MSK, Memorial Sloan Kettering Cancer Center; OS, overall survival; PFS, progression-free survival; TMB, tumour mutational burden; WT, wild-type.

associated with higher metastatic burden than wild-type cases, including brain metastases (Figure 2E and F). Together, these observations provided initial evidence that the VAF/TP ratio defines distinct types of *KEAP1* mutations.

KEAP1 clonality/LOH and clinical outcomes in LUAD patients treated with immunotherapy

Having shown that *KEAP1* C-LOH mutations have distinct clinical and genomic features, we aimed to determine whether these mutations were also associated with ICI efficacy. Baseline characteristics of patients included in this study are summarized in Supplementary Tables S3 and S4, available at https://doi.org/10.1016/j.annonc.2022.12.002, whereas the relationship between *KEAP1* mutations and baseline clinical features are provided in Supplementary Tables S5 and S6, available at https://doi.org/10.1016/j.annonc.2022.12.002.

In the MSK/Rome cohort, patients whose tumors harbored *KEAP1* C-LOH mutations had shorter PFS and OS compared to those with *KEAP1* wild-type diseases (PFS log-rank $P = 0.001$; OS log-rank $P < 0.001$, Figure 3A-D), whereas clinical outcomes were similar between patients with *KEAP1* CD-SC LUADs and those with *KEAP1* wild-type tumors.

Similarly, in the independent DFCI validation cohort, patients with *KEAP1* C-LOH LUADs had shorter PFS and OS compared to those with *KEAP1* wild-type tumors (PFS log-rank $P = 0.006$; OS log-rank $P = 0.014$, Figure 3E-H). Again, a similar association was not recorded for the *KEAP1* CD-SC group.

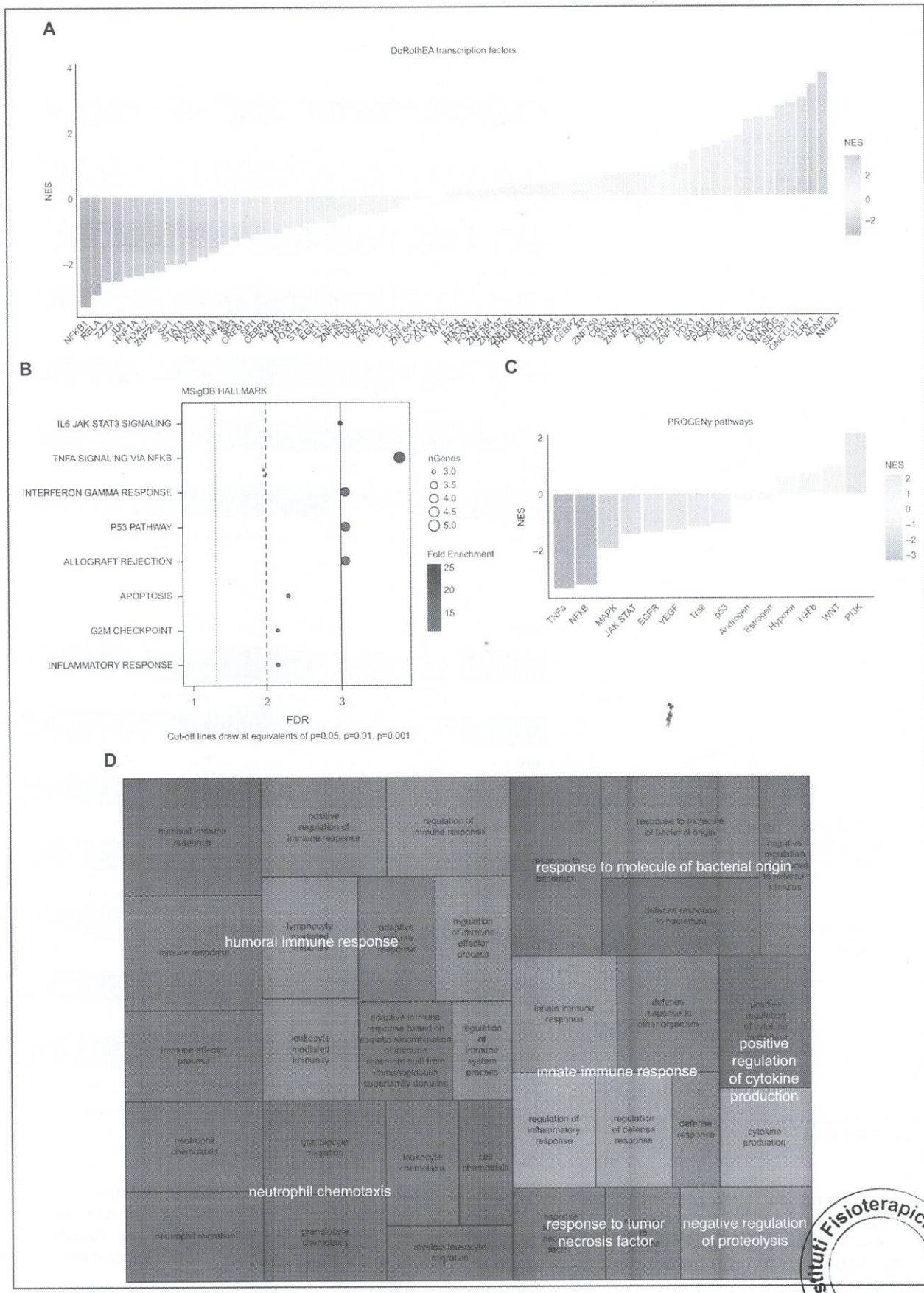

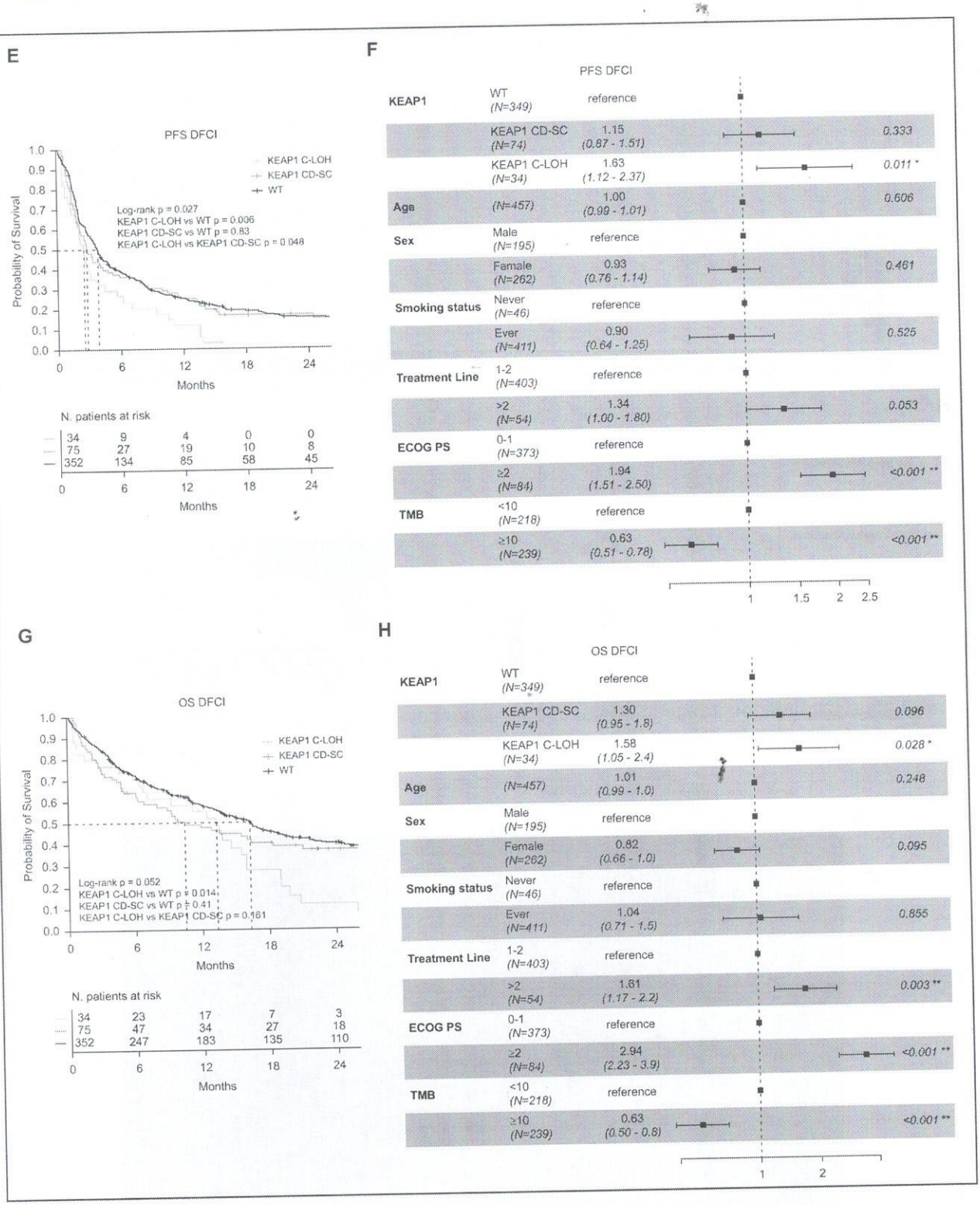

Figure 3. **Continued.**

PD-L1 expression [tumor proportion score (TPS)] was available in a subset of DFCI cases ($N = 371$). PD-L1 was lower among LUADs with *KEAP1* C-LOH compared to those with *KEAP1* CD-SC and *KEAP1* wild-type genotype (Supplementary Figure S4, available at https://doi.org/10.1016/j.annonc.2022.12.002). Multivariate Cox regression models confirmed the robustness of our classifier after adjusting for PD-L1 expression, indicating that our findings

are independent of PD-L1 (Supplementary Figure S5, available at https://doi.org/10.1016/j.annonc.2022.12.002). Moreover, the inclusion of patients with *EGFR*-activating mutations did not significantly impact our findings (Supplementary Figure S6, available at https://doi.org/10.1016/j.annonc.2022.12.002).

Lastly, we applied a similar approach to blood-based sequencing, exploiting the maximum somatic allele frequency (the amount of cell-free tumor DNA) as the counterpart of TP in liquid biopsy. In the OAK/POPLAR trials (atezolizumab arm), putative *KEAP1* C-LOH mutations were associated with worse PFS and OS compared to *KEAP1* CD-SC and *KEAP1* wild-type cases (Supplementary Figure S7, available at https://doi.org/10.1016/j.annonc.2022.12.002).[28] However, caution is needed in interpreting these data given the different sequencing strategies.

Pooled analysis of the immunotherapy-treated population

In order to account for inter-cohort variability in TP, we carried out a pooled analysis of the MSK/Rome/DFCI cohorts. All the tested VAF/TP cut-points were associated with an increased risk of disease progression and death (Supplementary Figure S8A and B, available at https://doi.org/10.1016/j.annonc.2022.12.002; highest tertile: VAF/TP $\geq$0.9). Also in the whole ICI-treated population, the VAF/TP ratio and TAPACLOTH achieved a comparable classification (Supplementary Figure S8C, available at https://doi.org/10.1016/j.annonc.2022.12.002). Regarding *TP53* mutations, these were more frequent in *KEAP1* C-LOH than *KEAP1* CD-SC tumors, as observed in the MSK MetTropism, even though this difference was not significant (Supplementary Figure S8D, available at https://doi.org/10.1016/j.annonc.2022.12.002). We next explored whether *KEAP1* C-LOH were associated with survival outcomes among TMB-high tumors. Differences in terms of PFS and OS were also observed in the TMB-high ($\geq$10) population (Supplementary Figure S8E and F, available at https://doi.org/10.1016/j.annonc.2022.12.002). The consistency of our model was further confirmed when a higher TMB cut-off ($\geq$19 mut/Mb) was considered (Supplementary Figure S9, available at https://doi.org/10.1016/j.annonc.2022.12.002).[29] However, the limited size of this TMB-high population ($N = 78$) hindered subgroup analyses.

Considering the link between *KEAP1* and *STK11*, we investigated *KEAP1/STK11* co-occurring complete inactivation (Supplementary Figure S10A, available at https://doi.org/10.1016/j.annonc.2022.12.002). Also when considering *STK11*, TAPACLOTH and the VAF/TP method yielded a comparable prediction (Supplementary Figure S10B, available at https://doi.org/10.1016/j.annonc.2022.12.002). By focusing on *KEAP1/STK11* co-mutant tumors, we noticed that ~65% of *KEAP1* C-LOH LUADs exhibited a common *STK11* pattern (Supplementary Figure S10C, available at https://doi.org/10.1016/j.annonc.2022.12.002). While patients with tumors having co-existing *KEAP1/STK11* C-LOH mutations had inferior survival outcomes compared to those with *KEAP1* CD-SC and wild-type tumors, we did not appreciate significant differences between *KEAP1/STK11* C-LOH and *KEAP1* C-LOH single-mutant tumors (Supplementary Figure S10D and E, available at https://doi.org/10.1016/j.annonc.2022.12.002). Even though we hypothesize a synergism between co-existing *KEAP1/STK11* C-LOH mutations, the limited sample size of the two *KEAP1*-mutant subgroups did not allow to further explore this relationship.

Next, we evaluated whether our classifier was affected by the number of metastatic sites. *KEAP1* C-LOH mutations were associated with shorter OS, regardless of metastatic burden (Supplementary Figure S11A and B, available at https://doi.org/10.1016/j.annonc.2022.12.002). Moreover, the distribution of the three molecular subgroups was not affected by the origin of the profiled tissues (primary versus metastatic tumors) (Supplementary Figure S11C, available at https://doi.org/10.1016/j.annonc.2022.12.002).

Lastly, we tested the impact of a common VAF/TP ratio cut-off ($\geq$0.9) in the two independent ICI-treated cohorts. Results were comparable in terms of survival outcomes (Supplementary Figure S12A-D, available at https://doi.org/10.1016/j.annonc.2022.12.002), even though a certain inter-cohort variability was observed in the distribution of VAF/TP values (Supplementary Figure S12E, available at https://doi.org/10.1016/j.annonc.2022.12.002).

Immunogenomic features associated with the different *KEAP1* mutations

Transcriptomic data (TCGA) were used to investigate differences in immune-related features across the three subgroups, classified with the same method used in clinical cohorts. TP estimates were fairly balanced between the two *KEAP1*-mutant groups (Supplementary Figure S13A, available at https://doi.org/10.1016/j.annonc.2022.12.002). This is relevant considering the impact of TP on sequencing-based immunological parameters (Supplementary Figure S13B and C, available at https://doi.org/10.1016/j.annonc.2022.12.002).

Transcription factor analysis (DoRothEA) revealed lower enrichment score of immune-related transcription factors in *KEAP1* C-LOH tumors as compared to *KEAP1* CD-SC cases (NFKB1/RELA, STAT1/STAT3) (Figure 4A). Consistently, transcription factor ontology, carried out with transcription factors having lower estimated activity in *KEAP1* C-LOH LUADs,

Figure 4. **Transcription factors and pathway-level analysis in the TCGA LUAD study.** Waterfall plot illustrating transcription factors (DoRothEA) differentially enriched when comparing *KEAP1* C-LOH and *KEAP1* CD-SC tumors (A). Gene ontology related to DoRothEA transcription factor analysis (MSigDB HALLMARK) (B). Waterfall plot for core pathway signatures (PROGENy) in *KEAP1* C-LOH versus *KEAP1* CD-SC LUADs (C). TreeMap plot displaying GSEA biological processes retrieved upon differential gene expression (*KEAP1* C-LOH versus *KEAP1* CD-SC tumors) (D).
CD-SC, clonal diploid-subclonal; C-LOH, clonal with loss of heterozygosity; GSEA, gene set enrichment analysis; LUAD, lung adenocarcinoma; NES, normalized enrichment score.

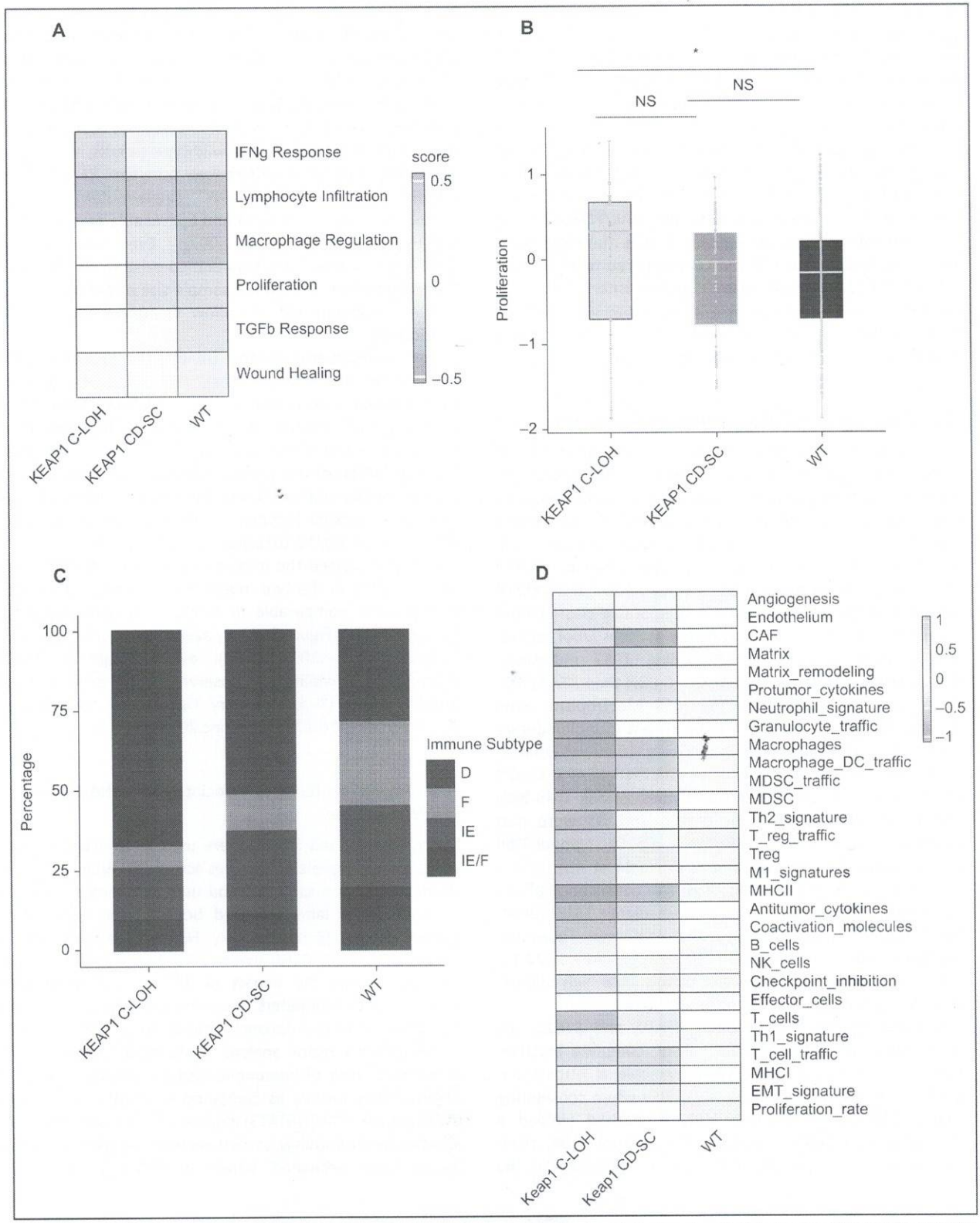

Figure 5. **Immune deconvolution and subtyping.** Heatmap of CRI iAtlas core immune-related signatures in the three investigated subgroups (*KEAP1* C-LOH, *KEAP1* CD-SC, and *KEAP1* wild-type) (A). Box plot related to the CRI iAtlas auxiliary proliferation signature (B). Stacked bar chart showing the distribution of conserved pan-cancer microenvironment subtypes in *KEAP1* C-LOH, *KEAP1* CD-SC, and *KEAP1* wild-type LUADs (C). Heatmap illustrating the 29 microenvironment-related signatures used for deriving the pan-cancer microenvironment subtyping (D). Asterisks indicate statistically significant differences.
CAF, cancer-associated fibroblast; CD-SC, clonal diploid-subclonal; C-LOH, clonal with loss of heterozygosity; D, desert (immune-depleted and non-fibrotic); EMT, epithelial-mesenchymal transition; F, fibrotic (immune-depleted and fibrotic); IE, immune-enriched and non-fibrotic; IE/F, immune-enriched and fibrotic; IFN-α, interferon gamma; MDSC, Myeloid-derived suppressor cells; MHC, major histocompatibility complex; NK, natural killer; NS, not significant; TGF-β, transforming growth factor-beta; WT, wild-type.

retrieved immune-related terms despite the limited size of input data (Figure 4B). The analysis of pathway-level signatures (PROGENy) indicated that *KEAP1* C-LOH tumors had lower enrichment scores of immune-associated pathways than *KEAP1* CD-SC LUADs (tumor necrosis factor-α, nuclear factor-κB, and Janus kinase/signal transducer and activator of transcription (JAK/STAT)) (Figure 4C). Conversely, the pro-proliferative PI3K signature was enriched in the *KEAP1* C-LOH group (Figure 4C). Gene ontology carried out with differentially expressed genes between the two *KEAP1*-mutant subgroups confirmed the downregulation of immune-related processes in *KEAP1* C-LOH versus *KEAP1* CD-SC LUADs (Figure 4D).

Next, we analyzed core immune signatures from a pan-cancer immunogenomic subtyping.[25] We observed differences across the subgroups, suggesting that an immune-cold microenvironment characterizes *KEAP1* C-LOH tumors (Figure 5A). Again, a signature denoting increased malignant potential (proliferation) was more represented in *KEAP1* C-LOH tumors (Figure 5B). Leveraging an independent compendium of immune-related processes,[26] we observed that *KEAP1* C-LOH LUADs were prevalently characterized by an immune-desert microenvironment, whereas immune enrichment was more common in *KEAP1* wild-type tumors (Figure 5C). In this context, *KEAP1* CD-SC LUADs had intermediate features. Interestingly, the two signatures enriched in the *KEAP1* C-LOH background were those associated with aggressive molecular traits (proliferation and epithelial-mesenchymal transition) (Figure 5D). Similarly, markers of genomic instability were more pronounced in the *KEAP1* C-LOH group than in *KEAP1* CD-SC LUADs (Supplementary Figure S14A-F, available at https://doi.org/10.1016/j.annonc.2022.12.002).

KEAP1 C-LOH tumors are associated with low immune cell infiltration

To further characterize the immunophenotypic features of *KEAP1* mutations, we exploited mIF in the independent DFCI mIF cohort ($N = 429$) (Figure 6A).

KEAP1 C-LOH mutations ($N = 17$) had fewer total CD8+ T cells compared to *KEAP1* CD-SC ($N = 38$) and *KEAP1* wild-type ($N = 374$) cases (Figure 6B). This association was prevalently driven by intratumoral CD8+ T cells (Supplementary Figure S15A and B, available at https://doi.org/10.1016/j.annonc.2022.12.002). *KEAP1* C-LOH tumors exhibited significantly lower total PD-1+ immune cells compared to *KEAP1* CD-SC and wild-type cases (Figure 6C), and a similar trend was reported for intratumoral PD-1+ immune cells (Supplementary Figure S15C and D, available at https://doi.org/10.1016/j.annonc.2022.12.002).

PD-L1 expression was lower among samples with *KEAP1* C-LOH mutations compared with those with *KEAP1* CD-SC and wild-type tumors, regardless of whether PD-L1 was classified with the TPS or the combined positive score (CPS) (Figure 6D and E).

Lastly, *KEAP1* C-LOH tumors had a numerically lower count of total CD8+ PD1+ T cells compared to *KEAP1* CD-SC and wild-type LUADs (Supplementary Figure S16A, available at https://doi.org/10.1016/j.annonc.2022.12.002). The exception was represented by FOXP3+ T cells, which were comparable across the three subgroups (Supplementary Figure S16D-F, available at https://doi.org/10.1016/j.annonc.2022.12.002).

Overall, mIF analysis confirmed that *KEAP1* C-LOH mutations are associated with an immune-excluded phenotype.

DISCUSSION

The advent of comprehensive genomic profiling in the clinical setting offers an unprecedented opportunity to gain insights into the taxonomy of tumors, and has prompted biology-informed clinical trials and biomarker identification studies.[23,30] In LUAD, evidence linking *KEAP1/STK11* mutations to survival outcomes are spurring intense debate on how to incorporate this information into clinical practice.[8,9,14,15,18,31] When considering immunotherapy, particular emphasis is placed on co-existing mutations in established drivers (*KRAS*, *TP53*, *KEAP1*, and *STK11*).[8,9,18,31] A growing body of evidence suggests that *KEAP1* mutations with or without concurrent alterations in genes such as *KRAS* and *STK11* are associated with resistance to PD-(L)1 blockade.[8,9,18] Nonetheless, responses to immunotherapy are also seen in patients with *KEAP1* mutations, regardless of their co-mutation background.

We hypothesized that *KEAP1* clonality/LOH prediction may help identify different classes of *KEAP1* mutations with distinct immunophenotypic features and clinical outcomes. We reported the following: (i) Patients with advanced LUADs who received ICIs and whose tumors carried putative *KEAP1* C-LOH mutations experienced inferior survival outcomes as compared to those with wild-type tumors. Conversely, survival outcomes of patients with *KEAP1* CD-SC tumors were similar to those having *KEAP1* wild-type LUADs; and (ii) *KEAP1* C-LOH LUADs exhibit an immune-cold tumor microenvironment.

Even though our results were reproducible in independent cohorts, we are aware that this study has some limitations. The main limitations stem from the retrospective design and the lack of information on PD-L1 expression, with the exception of the DFCI cohort. In this case, survival analyses carried out in the subset of DFCI patients with available PD-L1 data confirmed the stability of our classification. Moreover, we reported that tumors with *KEAP1* C-LOH mutations were characterized by low PD-L1 expression levels, and both computational studies in the TCGA and mIF data were aligned with this observation. In the DFCI cohort, the PD-L1-high (≥50%) population was slightly higher than that previously reported (DFCI 43.4%, KEYNOTE-024 30.2%).[32] This stems from the time frame of sample collection, and the evolution of immunotherapy-based therapeutic strategies over the same period (first-line pembrolizumab monotherapy in the PD-L1-high setting, first-line chemoimmunotherapy). The use of different sequencing strategies should also be considered. Even though we noticed some differences in sequencing coverage (Supplementary Figure S17A, available at https://doi.org/10.1016/j.annonc.2022.12.002), TAPACLOTH and the VAF/TP method had comparable performances when

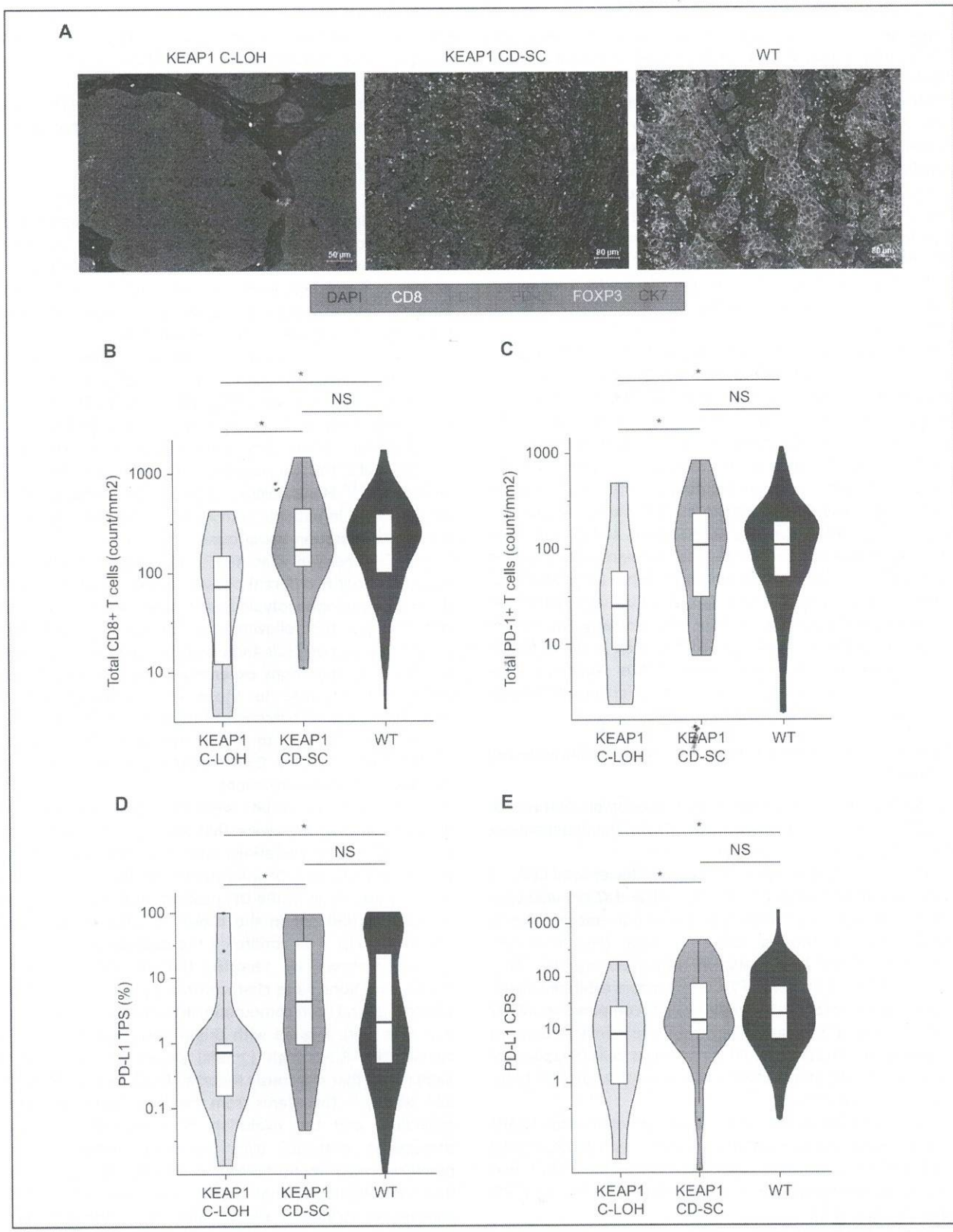

Figure 6. **Multiplexed immunofluorescence (mIF) in DFCI LUAD cases.** Three representative images (*KEAP1* C-LOH, *KEAP1* CD-SC, and *KEAP1* wild-type) of LUAD samples characterized by mIF at the DFCI (ImmunoProfile) (A). Violin plots for total CD8+ T cells (B), total PD-1+ T cells (C), and PD-L1 (D and E). CD-SC, clonal diploid-subclonal; C-LOH, clonal with loss of heterozygosity; CPS, combined positive score; DFCI, Dana-Farber Cancer Institute; DAPI, 4′,6-diamidino-2-phenylindole; LUAD, lung adenocarcinoma; NS, not significant; PD-1, programmed cell death protein 1; PD-L1, programmed death-ligand 1; TPS, tumor proportion score; WT, wild-type. Asterisks indicate statistically significant differences.

the two ICI-treated cohorts were separately analyzed, indicating that our methods are not affected by the sequencing platforms (Supplementary Figure S17B, available at https://doi.org/10.1016/j.annonc.2022.12.002). We also considered the potential impact of clonal hematopoiesis (CH), a source of mutation misinterpretation in tumor-only sequencing.[33] However, publicly available data indicate that CH-associated *KEAP1* mutations are extremely uncommon (<0.1%).[34] Lastly, our study was not powered to explore the impact of the different *KEAP1* classes according to *KRAS* status.[18]

At the same time, our findings have some important implications. Firstly, our method significantly widens the amount of information achievable in clinical targeted sequencing, ensuring the flexibility to be transferred to other treatments (e.g. $KRAS^{G12C}$ inhibition), settings (neo-adjuvant/adjuvant), and tumor types. In addition, the results of our study may open new horizons in the search of anti-immune interactions,[35] and can improve current mutational co-occurrence approaches. Indeed, incorporating clonality/LOH into mutational co-occurring models is expected to increase our ability to delineate the genomic repertoire of tumors with an enhanced capability of evading the immune system. Introducing the clonal status of driver mutations may also generate a more detailed molecular segmentation of the disease with important therapeutic implications (treatment intensification, clinical trials). A more granular interpretation of clinical sequencing data would allow to narrow the pool of clinically relevant genes and alterations, eliminating the background noise of clinically neutral mutations. Intuitively, our data highlight the importance of integrating CNAs in clinical practice. From a clinical perspective, *KEAP1* clonal status may frame *KEAP1*-mutant LUADs responding to ICIs. Currently, there are multiple first-line options, including PD-(L)1 monotherapy, PD-(L)1 plus cytotoxic T-lymphocyte-associated protein 4 dual blockade, and chemoimmunotherapy. While chemoimmunotherapy is usually favored in the presence of low/intermediate PD-L1 expression, there are no prospective data guiding treatment decision for patients with PD-L1-high (≥50%) tumors. Our data suggest that tumors with *KEAP1* C-LOH mutations are particularly refractory to PD-(L)1 monotherapy. Therefore, combination approaches might be considered for this population. Conversely, patients with tumors carrying *KEAP1* CD-SC mutations have similar outcomes to those with *KEAP1* wild-type LUADs. Among patients with tumors exhibiting high PD-L1 expression and *KEAP1* CD-SC mutations, single-agent PD-(L)1 inhibitors may be considered, sparing the added toxicity of chemotherapy. While other features must be factored in this decision (age, performance status, disease burden), our study indicates that *KEAP1* status may help individualizing treatment selection.

From a methodological perspective, we observed slightly different median TP values in the examined cohorts, which is a common scenario in clinical practice. Given the overlap between TAPACLOTH and the VAF/TP method, we were able to harmonize the cohorts in terms of clonality/LOH prediction. Nevertheless, introducing standardized procedures for TP estimation is of key relevance to foster the implementation of these models in clinical sequencing.[36-38] The increased throughput of targeted sequencing, and the reduced costs of WES, will offer the opportunity to develop more efficient TP estimation methods (combined pathologist-estimated and inferred TP, digital pathology).[36-38] Secondly, clonal deconvolution is still in its initial phase, as denoted by the inconsistencies reported across the various tools that reconstruct clonal architecture.[39] Bringing this concept to clinical sequencing remains a challenging, albeit promising, task.

In summary, we provided evidence that clonality/LOH prediction in clinical sequencing allows to identify advanced *KEAP1*-mutant LUAD patients experiencing less favorable survival outcomes when treated with ICIs. These data invite caution when administering ICIs to patients with tumors harboring a certain type of *KEAP1* alterations, regardless of co-existing mutations. Testing this hypothesis in prospective studies and in the chemoimmunotherapy setting will be instrumental in assessing the potential of second-generation genomic classifiers.

ACKNOWLEDGEMENTS

We thank Tania Merlino for her editorial assistance.

FUNDING

This work was supported by the Italian Association for Cancer Research (AIRC) under MFAG 2019 [grant number 22940 to MMS], and the Italian Ministry of Health (MoH) [grant number GR-2016-02362025 to MMS]. The Conquer Cancer Foundation of the American Society for Clinical Oncology and the Society for Immunotherapy of Cancer [to BR]. The Italian Association for Cancer Research (AIRC) under MFAG 2020 [grant number 24913 to GC and NC].

DISCLOSURE

PV reports travel grants from Eisai, Roche, Pfizer, Novartis; speaker fees/advisory boards from Roche, Pfizer, Novartis, Gentili. RDM reports serving as a scientific advisory board member at Exosomics SpA (Siena IT), HiberCell Inc. (New York, NY), Kiromic Inc. (Houston, TX) and Exiris Inc. (Rome, IT). FC reports personal fees from Roche/Genentech, AstraZeneca, Takeda, Pfizer, Bristol-Myers Squibb, Merck Sharp & Dohme, Lilly, and Bayer. MMA reported serving as a consultant for Achilles, AbbVie, Neon, Maverick, Nektar, and Hegrui; receiving grants and personal fees from Genentech, Bristol-Myers Squibb, Merck, AstraZeneca, and Lilly; and receiving personal fees from Maverick, Blueprint Medicine, Syndax, Ariad, Nektar, Gritstone, ArcherDx, Mirati, NextCure, Novartis, EMD Serono, and NovaRx. All other authors have declared no conflicts of interest.

DATA SHARING

Data concerning the Rome cohort are disclosed in our previous work.[8] MSK studies are available at www.

cbioportal.org. The DFCI cohort is available from the authors upon reasonable request (B. Ricciuti and M.M. Awad).

REFERENCES

1. Pillai R, Hayashi M, Zavitsanou AM, Papagiannakopoulos T. NRF2: KEAPing tumors protected. *Cancer Discov*. 2022;12:625-643.
2. Hellyer JA, Padda SK, Diehn M, Wakelee HA. Clinical implications of KEAP1-NFE2L2 mutations in NSCLC. *J Thorac Oncol*. 2021;16:395-403.
3. Scalera S, Mazzotta M, Cortile C, et al. KEAP1-Mutant NSCLC: the catastrophic failure of a cell-protecting hub. *J Thorac Oncol*. 2022;17:751-757.
4. Marzio A, Kurz E, Sahni JM, et al. EMSY inhibits homologous recombination repair and the interferon response, promoting lung cancer immune evasion. *Cell*. 2022;185:169-183.e19.
5. Kitamura H, Onodera Y, Murakami S, Suzuki T, Motohashi H. IL-11 contribution to tumorigenesis in an NRF2 addiction cancer model. *Oncogene*. 2017;36:6315-6324.
6. Kobayashi EH, Suzuki T, Funayama R, et al. Nrf2 suppresses macrophage inflammatory response by blocking proinflammatory cytokine transcription. *Nat Commun*. 2016;7:11624.
7. Olagnier D, Brandtoft AM, Gunderstofte C, et al. Nrf2 negatively regulates STING indicating a link between antiviral sensing and metabolic reprogramming. *Nat Commun*. 2018;9:3506.
8. Marinelli D, Mazzotta M, Scalera S, et al. KEAP1-driven co-mutations in lung adenocarcinoma unresponsive to immunotherapy despite high tumor mutational burden. *Ann Oncol*. 2020;31:1746-1754.
9. Scalera S, Mazzotta M, Corleone G, et al. KEAP1 and TP53 frame genomic, evolutionary, and immunologic subtypes of lung adenocarcinoma with different sensitivity to immunotherapy. *J Thorac Oncol*. 2021;16:2065-2077.
10. Cancer Genome Atlas Research Network. Comprehensive molecular profiling of lung adenocarcinoma. *Nature*. 2014;511:543-550.
11. Cerami E, Gao J, Dogrusoz U, et al. The cBio cancer genomics portal: an open platform for exploring multidimensional cancer genomics data. *Cancer Discov*. 2012;2:401-404.
12. Gao J, Aksoy BA, Dogrusoz U, et al. Integrative analysis of complex cancer genomics and clinical profiles using the cBioPortal. *Sci Signal*. 2013;6:pl1.
13. Singh A, Misra V, Thimmulappa RK, et al. Dysfunctional KEAP1-NRF2 interaction in non-small-cell lung cancer. *PLoS Med*. 2006;3:e420.
14. Goeman F, De Nicola F, Scalera S, et al. Mutations in the KEAP1-NFE2L2 pathway define a molecular subset of rapidly progressing lung adenocarcinoma. *J Thorac Oncol*. 2019;14:1924-1934.
15. Binkley MS, Jeon YJ, Nesselbush M, et al. KEAP1/NFE2L2 mutations predict lung cancer radiation resistance that can be targeted by glutaminase inhibition. *Cancer Discov*. 2020;10:1826-1841.
16. Foggetti G, Li C, Cai H, et al. Genetic determinants of EGFR-driven lung cancer growth and therapeutic response in vivo. *Cancer Discov*. 2021;11:1736-1753.
17. Krall EB, Wang B, Munoz DM, et al. KEAP1 loss modulates sensitivity to kinase targeted therapy in lung cancer. *Elife*. 2017;6:e18970.
18. Ricciuti B, Arbour KC, Lin JJ, et al. Diminished efficacy of PD-(L)1 inhibition in STK11- and KEAP1-mutant lung adenocarcinoma is impacted by KRAS mutation status. *J Thorac Oncol*. 2022;17:399-410.
19. Roth A, Khattra J, Yap D, et al. PyClone: statistical inference of clonal population structure in cancer. *Nat Methods*. 2014;11:396-398.
20. Cun Y, Yang TP, Achter V, et al. Copy-number analysis and inference of subclonal populations in cancer genomes using Sclust. *Nat Protoc*. 2018;13:1488-1501.
21. Caravagna G, Heide T, Williams MJ, et al. Subclonal reconstruction of tumors by using machine learning and population genetics. *Nat Genet*. 2020;52:898-907.
22. Caravagna G, Giarratano Y, Ramazzotti D, et al. Detecting repeated cancer evolution from multi-region tumor sequencing data. *Nat Methods*. 2018;15:707-714.
23. Samstein RM, Lee CH, Shoushtari AN, et al. Tumor mutational load predicts survival after immunotherapy across multiple cancer types. *Nat Genet*. 2019;51:202-206.
24. Rizvi H, Sanchez-Vega F, La K, et al. Molecular determinants of response to anti-programmed cell death (PD)-1 and anti-programmed death-ligand 1 (PD-L1) blockade in patients with non-small-cell lung cancer profiled with targeted next-generation sequencing. *J Clin Oncol*. 2018;36:633-641.
25. Thorsson V, Gibbs DL, Brown SD, et al. The immune landscape of cancer. *Immunity*. 2018;48:812-830.e14.
26. Bagaev A, Kotlov N, Nomie K, et al. Conserved pan-cancer microenvironment subtypes predict response to immunotherapy. *Cancer Cell*. 2021;39:845-865.e7.
27. Bogusz AM, Baxter RH, Currie T, et al. Quantitative immunofluorescence reveals the signature of active B-cell receptor signaling in diffuse large B-cell lymphoma. *Clin Cancer Res*. 2012;18:6122-6135.
28. Gandara DR, Paul SM, Kowanetz M, et al. Blood-based tumor mutational burden as a predictor of clinical benefit in non-small-cell lung cancer patients treated with atezolizumab. *Nat Med*. 2018;24:1441-1448.
29. Ricciuti B, Wang X, Alessi JV, et al. Association of high tumor mutation burden in non-small cell lung cancers with increased immune infiltration and improved clinical outcomes of PD-L1 blockade across PD-L1 expression levels. *JAMA Oncol*. 2022;8:1160-1168.
30. Nguyen B, Fong C, Luthra A, et al. Genomic characterization of metastatic patterns from prospective clinical sequencing of 25,000 patients. *Cell*. 2022;185:563-575.e11.
31. Skoulidis F, Goldberg ME, Greenawalt DM, et al. STK11/LKB1 mutations and PD-1 inhibitor resistance in KRAS-mutant lung adenocarcinoma. *Cancer Discov*. 2018;8:822-835.
32. Reck M, Rodriguez-Abreu D, Robinson AG, et al. Pembrolizumab versus chemotherapy for PD-L1-positive non-small-cell lung cancer. *N Engl J Med*. 2016;375:1823-1833.
33. Coombs CC, Gillis NK, Tan X, et al. Identification of clonal hematopoiesis mutations in solid tumor patients undergoing unpaired next-generation sequencing assays. *Clin Cancer Res*. 2018;24:5918-5924.
34. Bolton KL, Ptashkin RN, Gao T, et al. Cancer therapy shapes the fitness landscape of clonal hematopoiesis. *Nat Genet*. 2020;52:1219-1226.
35. Etxeberria I, Teijeira A, Montuenga LM, et al. Epistatic oncogenic interactions determine cancer susceptibility to immunotherapy. *Cancer Discov*. 2018;8:794-796.
36. Haider S, Tyekucheva S, Prandi D, et al. Systematic assessment of tumor purity and its clinical implications. *JCO Precis Oncol*. 2020;4:00016. PO.20.
37. Aran D, Sirota M, Butte AJ. Systematic pan-cancer analysis of tumour purity. *Nat Commun*. 2015;6:8971.
38. Brendel M, Getseva V, Al Assaad M, et al. Weakly-supervised tumor purity prediction from frozen H&E stained slides. *EBioMedicine*. 2022;80:104067.
39. Tanner G, Westhead DR, Droop A, Stead LF. Benchmarking pipelines for subclonal deconvolution of bulk tumour sequencing data. *Nat Commun*. 2021;12:6396.